A NOVEL HIGH-SPEED PIEZOELECTRIC DEFORMABLE VARIFOCAL MIRROR FOR OPTICAL APPLICATIONS

Mark J. Mescher*, Michael L. Vladimer*, Jonathan J. Bernstein**
*Charles Stark Draper Laboratory, Cambridge, MA
**IntelliSense Corp., Wilmington, MA

Abstract – **We describe the characteristics of a microelectromechanical deformable optical component: a parabolic focusing mirror having a focal length that is controlled by piezoelectric actuation of thin-film PZT. Devices of two different sizes were tested and have resonant frequencies in the low MHz range, nominal focal lengths between 1500 and 2000 μm and numerical apertures of approximately 0.10 and 0.05. Tuning ranges of several hundred microns have been demonstrated. Finite element modeling is described and compared to measured results. The equations required for device scaling are provided to show some of the tradeoffs that can be made between aperture size, mechanical bandwidth and focal length tuning range.**

I. INTRODUCTION

The capability of current large-scale deformable-optics devices is limited by the large stiffness in typical macro- or mini-mirrors caused by the appreciable thickness of the actuator and mirror layers [1]- [5]. Much larger changes in focal length can be achieved if this stiffness is reduced. Electrostatically actuated devices have been demonstrated [6], [7]. These devices must avoid electrostatic pull-in onto a planar electrode in order to maintain constant curvature of the focusing element. As a result, gaps may be large and forces small. Small electrostatic forces necessitate the use of relatively compliant membranes for the mirrors, which thus limits their mechanical bandwidth. In addition, the non-linear forces generated by the non-uniform gap typically present in such devices will result in non-uniform bending of the plate. The multi-electrode schemes used to compensate for this distortion add additional complexity, particularly when curvature uniformity is required over a large tuning range. Another mechanism that provides adaptive focusing uses a lens that translates along the optical axis relative to other lenses in the path, thus changing focal length. These systems are also typically slow because of the mass of the components. Thin film piezoelectric technology provides both the decrease in mass and the necessary forces required to deform relatively stiff plates required to achieve high-frequency deformable optical components. Specifically, it can be used to alter the buckled state of a MEMS-machined thin-film plate. Upon application of voltage to the piezoelectric layer, lateral strain is generated which changes the membrane buckling and thus the mirror curvature, as shown in Figure 1. While piezo-actuated micro-mirrors have been have used in conjunction with macro-scale lenses to achieve focusing devices [8], high-speed micro-lenses with tunable focal lengths have not before been implemented. A high-speed deformable focusing element could provide new capabilities in numerous applications, including sample height variation compensation in scanning confocal microscopy, vibration compensation, and collimation correction of poorly collimated beams in optical switching applications where path lengths change.

A key requirement for fabricating controlled-buckle membranes is the control of the residual stresses in the thin films making up the membrane [9]. These stresses determine the initial curvature of the mirror structure and are thus important in determining the tuning range in which a particular mirror can operate. Further, the thickness and lateral dimensions control the degree of buckling for given residual stresses and applied excitation voltage.

The performance characteristics of the lens structure are strongly dependent upon various design parameters, including total and relative film thickness, and the radii of the mirror membrane and piezoelectric ring actuator. Finite Element Analysis was used to model performance characteristics. The various trade-offs between tuning range, tuning linearity, and maximum operating frequency are described. A comparison with experimental results is presented.

0-7803-7185-2/02/$10.00 ©2002 IEEE

II. DEVICE STRUCTURE

The basic structure consists of a circular membrane released by a backside deep-RIE through-wafer etch, as shown in Figures 2. The top surface of the membrane has a ring-shaped piezoelectric actuation layer, as shown in Figure 3. This iris-shaped structure is composed of a sol-gel "monomorph" PZT layer as the active piezoelectric deposited on insulating layers of ZrO_2 and SiO_2 on a polysilicon structural layer. An in-plane polarization scheme which makes use of the d_{33} rather than d_{31} piezoelectric coefficient of the PZT is used to maximize tunability, as described in [10] and shown in Figure 4 (d_{33}, at approximately 200pm/V, is typically at least twice as large as d_{31} for PZT [11]). This in-plane scheme results in an important design tradeoff that must be considered. Because the capacitor formed by this configuration has small cross-sectional area (film thickness x electrode length) and large dielectric gap (electrode spacing) the capacitance can be made very small, at the expense of requiring a large voltage to induce a sufficiently large electric field. Because these devices were tested only to show feasibility, no particular set of input voltage and impedance requirements were considered. The two sizes of structures tested both measured capacitances of approximately 0.7pF.

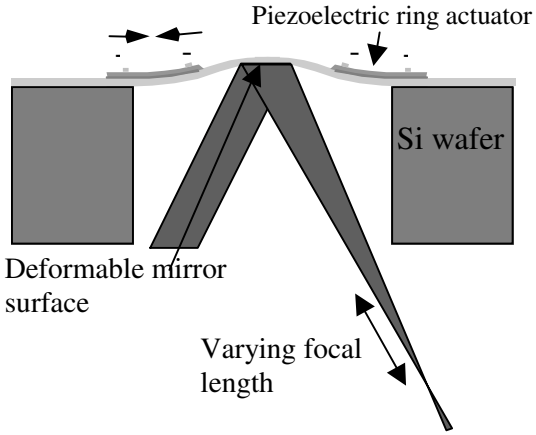

Figure 1. Cross section of variable focal length mirror.

Details of the fabrication are also described in [10]. Table 1 shows the film thickness and residual stress of the plate layer, which was composed of thermal oxide, polysilicon, LTO (low temperature oxide), and insulating ZrO_2, and the piezoelectric layer. The piezoelectric was deposited by sol-gel process at Penn State University [11].

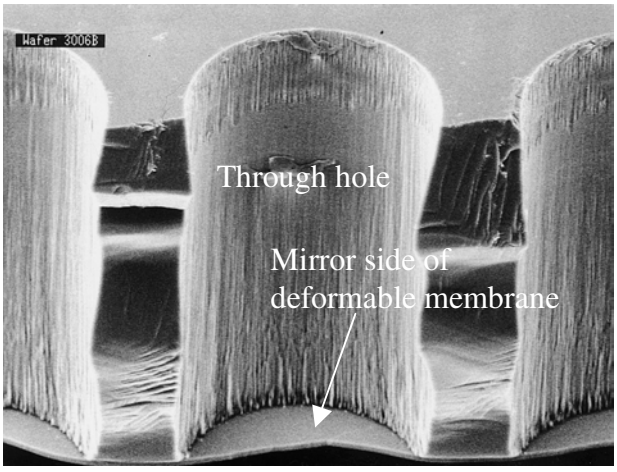

Figure 2. Cross-section SEM of circular mirror membrane and backside through-hole deep RIE etch(diameter = 300μm).

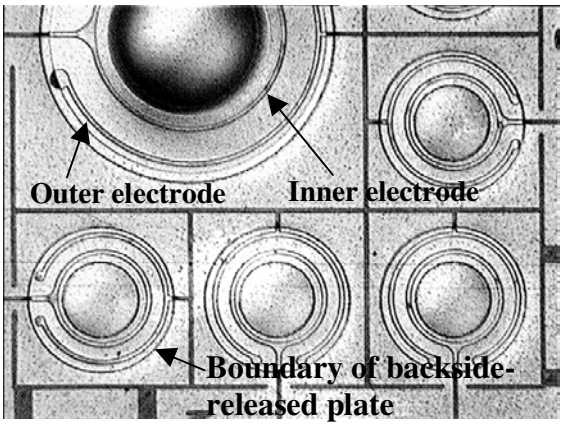

Figure 3. Top-view micrograph of the two different sizes of fabricated lenses. Mirror surface is opposite face [10].

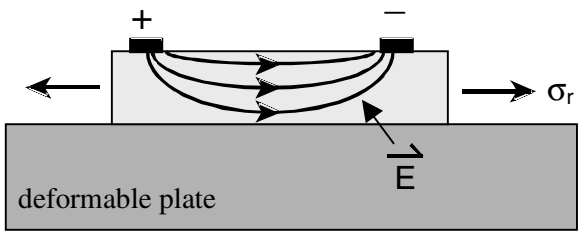

Figure 4. Cross sectional schematic of in-plane excitation of PZT thin film actuator and induced bending moment.

Table 1. Device parameters used for FEM modeling. (C – compressive, T – tensile)

Material	Thickness [μm]	Approx. Avg. Young's modulus [GPa]	Residual stress [MPa]
SiO_2/Si/ SiO_2/ZrO_2	1.5/2.8/ 1.5/ 0.5	100	300 C
PZT	2.7	80	75 T

III. MEASUREMENT

Surface profiles of the membranes were taken with an RST-Plus Wyko Optical Profiler. Typical 3-D renderings are shown in Figure 5. A series of deflection profiles are shown in Figure 6 by extracting a portion of the data corresponding to a single cross section that runs through the center of the mirror. Each trace is taken at a different actuator excitation voltage.

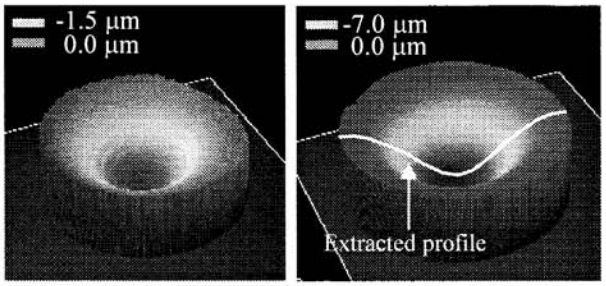

Figure 5. Measured 2 – D profiles. Left: radius = 150μm. Right: radius = 300μm.

Data analysis of the resulting curves yielded the sizes of the region of the deformable mirrors that would serve to focus light with little or no aberration. The criterion used for selecting this effective diameter or aperture size was a correlation corresponding to $R^2 > 0.99$ between a parabolic fit and the measured data over the fitted interval. For both sizes of mirrors tested, this diameter was very close to one half the total diameter of the thin film plate. Thus the effective apertures for the two devices were 150 and 300μm.

IV. FINITE ELEMENT MODEL

Finite element modeling was used to examine the small-radius device. As seen in Figures 5 and 6, the nominal deflection of the large device was approximately 7.2μm. Given a total membrane thickness of 6.3μm, this device is in a buckled state. The available FEM tool (CoventorWare© 2001.3) does not provide buckling analysis; the numerical analysis of the large-diameter device was not undertaken.

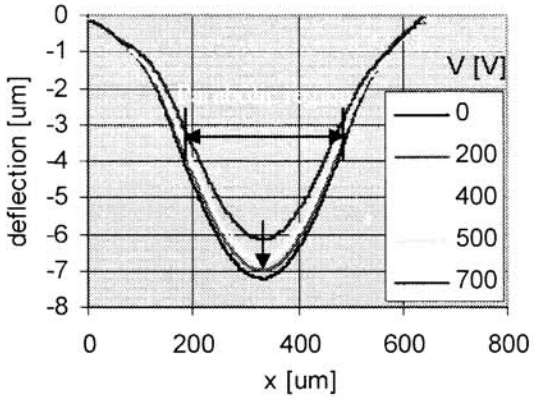

Figure 6. Measured displacement profile across mirror center extracted from 3-D profile interferometer images. Each trace represents a different applied tuning voltage.

The nominal curvature resulting from residual thin film stresses in the released thin film plates and the focal length tuning sensitivity and linearity were the primary parameters analyzed. Measurements of cantilever deflections of the materials in the full plate (the insulators and polysilicon) and the piezoelectric ring layer yielded approximate average residual stress values for these composite layers as listed in Table 1. These values were initially used (applied as a zero-order term in the "Stress-gradient" field to achieve uniform plane strain. and resulted in plate deflections that matched experimental within 30%. Modification of the residual PZT stress value allowed the residual stress-solutions to be matched exactly with experimentally obtained data. The addition of piezoelectrically actuated stress was accomplished by adding an additional residual plane stress to the PZT region between the electrodes having a value

$$(1)\quad \sigma_{PZT} = \frac{Y}{1-\upsilon^2} d_{33} E_r$$

where Y is Young's modulus, υ the Poisson ratio, and E_r the radial applied field. This is depicted in the solid model drawing of Figure 7 by the dark band shown within the PZT ring. The electrode spacing for the modeled device was 40μm.

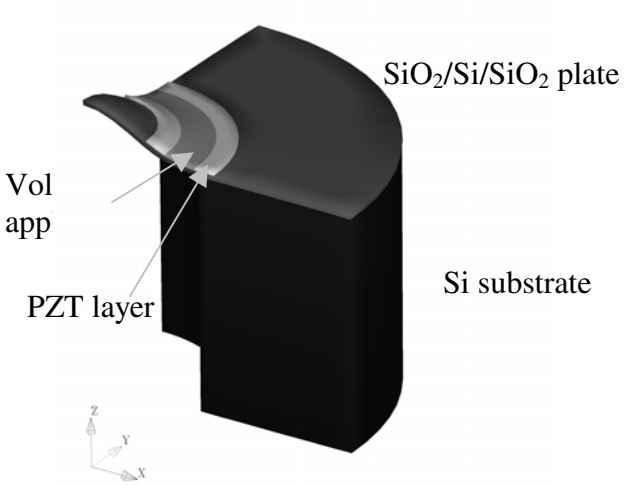

Figure 7. Quarter-symmetry model used in CoventorWare for deflection modeling

V. RESULTS

Results are plotted in Figures 8 and 9. Both device types demonstrate excellent linearity. There is also excellent agreement between the measured and predicted tuning sensitivity with applied voltage, as shown in Figure 9. Measurements on multiple devices are included in the plot. Each experimental data point represents the average focal length obtained by taking an x- and y- cross section of the 3-D interferometer data. Some of the scatter is a result of the decreased signal to noise of the measurement, given the much smaller absolute displacements of the small devices relative to the larger (maximum of approximately 1.0μm vs. 7.2μm).

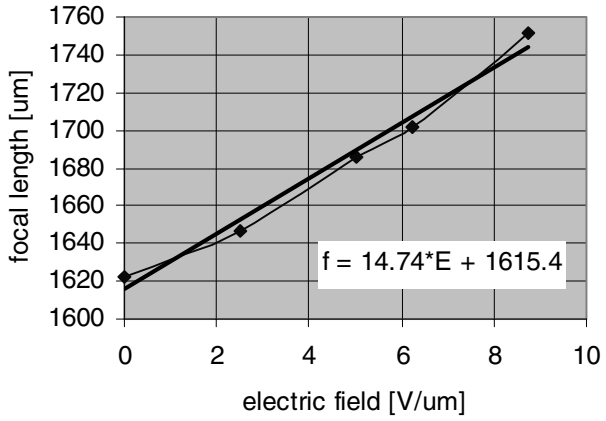

Figure 8. Measured focus change as a function of applied voltage for the R=300μm deformable mirror.

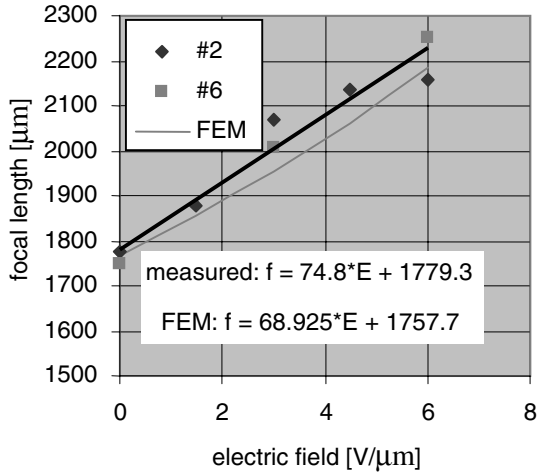

Figure 9. Measured vs. FEM simulation of focal length as a function of applied electric field. Experimental data points are from two distinct devices (R = 150μm).

In order to examine the effects of changes in size of this type of mirror (both film thickness and plate diameter) we present an approximate deflection formula that includes both bending and built-in residual stresses, but for circular membranes of uniform cross section. This is sufficient to allow for basic scaling analysis. More complex analysis is required to achieve to achieve quantitative results. For relatively small deflections, the deflection shape of a circular plate can be represented by [12][13]

$$(2)\quad z = \frac{PR^4}{64D}\frac{1}{1+\frac{\sigma t}{16D}(R^2-r^2)}\left[1-(\frac{r}{R})^2\right]^2$$

where P is an applied uniform pressure load, R is the plate radius, σ is the residual in-plane stress, r is the radius variable, and

$$(3)\quad D = \frac{Yt^3}{12(1-\upsilon^2)}$$

is the flexural rigidity. While a normal load P is not applied to the deformable membrane, this constant can be used as a fitting parameter to scale the equation given at least one known data point. Changes in plate thickness or radius can then be applied to calculate an approximate nominal

residual deflection for a device of different thickness and diameter.

VI. CONCLUSIONS

We have measured the nominal focal length and tuning sensitivity of two sizes of micromachined deformable mirrors. The measured data shows reasonable correlation with plate bending solutions generated from finite element models. The substantial tuning range and speed suggest that this type of deformable optical component may be applied to applications where rapid focal length tuning is a requirement. Quantifying the extent to which fabricating thinner devices for larger tuning range will degrade optical focusing capability (due to non-uniform curvature) will require an analysis of fabrication tolerances, including film thickness uniformity and homogeneity. Future work in modeling will more precisely determine the tradeoffs in design that result in optimized performance for a given application.

ACKNOWLEDGEMENT

The authors acknowledge support from the following people: Amy Duwel, Bill Kelleher and Francis Rogomentich.

REFERENCES

[1] N. T. Adelman, "Spherical Mirror With Piezoelectrically Controlled Curvature," *Applied Optics* **16**, 3075 – 75, December 1977.

[2] E. Steinhaus and S. G. Lipson, "Bimorph Piezoelectric Flexible Mirror," *J. Opt. Soc. Am*. **69**, 487 – 481, March 1979.

[3] S. A. Kokorowski, "Analysis of Adaptive Optical Elements made from Piezoelectric Bimorphs," *J. Opt. Soc. Am.* **69**, 181 – 187, Jan. 1979.

[4] T. Sato, et. al. "Multilayered Deformable Mirror Using PVDF Films," *Applied Optics* **21**, 3664 – 68, 15 October 1982.

[5] T. Sato, et. al. "Deformable 2-D Mirror Using Multilayered Electrostrictros," *Applied Optics* **21,** 3669 – 72, 15 October 1982.

[6] L.M. Miller, et. al., "Fabrication And Characterization of Micromachined Deformable Mirror For Adaptive Optics Applications," *Proc. SPIE* **1954**, 421-430 (1993).

[7] G.V. Vdovin and P.M. Sarro, "Flexible mirror micromachined in silicon," *Applied Optics* **34,** 2968-2972 (1995).

[8] M. Sakata, et. al. "Basic Characteristics of a Piezoelectric Buckling Type of Actuator," *The Eighth International Conference on Solid-State Sensors and Actuators – Transducers* '95, Stockholm, Sweeden, 25-29 June 1995.

[9] M. Mescher, et. al. "Variable Focal Length Microelectromechanical Lens", *SPIE - The International Society for Optical Engineering Conference,* Vol. 3289 , 1998, 171-6.

[10] J.J. Bernstein, J. Bottari, et. al., "Advanced MEMS Ferroelectric Ultrasound 2D Arrays" *IEEE Ultrasonics Symposium*, vol.2 , 1145-53, 1999.

[11] K. R. Udayakumar et. al., "Ferroelectric Thin Film Ultrasonic Micromotors," *Proceedings of the 4th IEEE Workshop on MicroElectroMechanical Systems (MEMS-91),* Nara, Japan, 109 – 113, 1991.

[12] W. P. Eaton IV, "Surface Micromachined Pressur Sensors, Doctoral Thesis, Univ. New Mexico, p. 112, 1997.

[13] R. Schellin, et. al., "Measurements Of The Mechanical Behavior Of Micromachined Silicon And Silicon-Nitride Membranes For Microphones, Pressure Sensors, And Gas Flow Meters," *Sensors and Actuators A* **41-42**, 287-292 (1994).